BioSystems 118 (2014) 51–59

Contents lists available at ScienceDirect

BioSystems

journal homepage: www.elsevier.com/locate/biosystems

Within-host influenza dynamics: A small-scale mathematical modeling approach

Himanshu Manchanda[a,b,1], Nora Seidel[b,1], Andi Krumbholz[b,c], Andreas Sauerbrei[b], Michaela Schmidtke[b,*], Reinhard Guthke[a,**]

[a] Leibniz Institute for Natural Product Research and Infection Biology – Hans Knöll Institute, Jena, Germany
[b] Jena University Hospital, Department of Virology and Antiviral Therapy, Jena, Germany
[c] Institute for Infection Medicine, Christian-Albrecht University of Kiel and University Medical Center Schleswig-Holstein, Campus Kiel, Kiel, Germany

ARTICLE INFO

Article history:
Received 28 June 2013
Received in revised form 24 February 2014
Accepted 27 February 2014
Available online 11 March 2014

Keywords:
Influenza virus
Infection
Modeling
Virus replication
Immune response
Inflammation

ABSTRACT

The emergence of new influenza viruses like the pandemic H1N1 influenza A virus in 2009 (A(H1N1)pdm09) with unpredictable difficulties in vaccine coverage and established antiviral treatment protocols emphasizes the need of new murine models to prove the activity of novel antiviral compounds *in vivo*. The aim of the present study was to develop a small-scale mathematical model based on easily attainable experimental data to explain differences in influenza kinetics induced by different virus strains in mice. To develop a three-dimensional ordinary differential equation model of influenza dynamics, the following variables were included: (i) viral pathogenicity (P), (ii) antiviral immune defense (D), and (iii) inflammation due to pro-inflammatory response (I). Influenza virus-induced symptoms (clinical score S) in mice provided the basis for calculations of P and I. Both, mono- and biphasic course of mild to severe influenza induced by three clinical A(H1N1)pdm09 strains and one European swine H1N2 virus were comparatively and quantitatively studied by fitting the mathematical model to the experimental data. The model hypothesizes reasons for mild and severe influenza with mono- as well as biphasic course of disease.

According to modeling results, the second peak of the biphasic course of infection is caused by inflammation. The parameters (i) maximum primary pathogenicity, (ii) viral infection rate, and (iii) rate of activation of the immune system represent most important parameters that quantitatively characterize the different pattern of virus-specific influenza kinetics.

1. Introduction

In April 2009 a new pandemic H1N1 influenza A virus (A(H1N1)pdm09) emerged (Dawood et al., 2009; Ginsberg et al., 2009). It replaced seasonal H1N1 viruses and continued to circulate together with H3N2 and influenza B viruses causing millions of infections per year (WHO, 2013).

A(H1N1)pdm09 virus is M2 ion channel blocker-resistant and neuraminidase (NA) inhibitor (NAI)-sensitive (Dawood et al., 2009; Gubareva et al., 2009). However, since its emergence several mutations were identified that resulted in reduced NAI susceptibility or even resistance (Nguyen et al., 2012). Moreover, A(H1N1)pdm09 virus lacks the 150-cavity that is typical of group 1 NA (Li et al., 2010) and presents a structurally new target for the development of new inhibitory compounds (Kirchmair et al., 2011). In addition, the virus has a natural resistance against the potential nucleoprotein inhibitor nucleozin (Kao et al., 2010). Thus, there is an urgent need for the development of new anti-influenza compounds.

The efficacy of novel potential drug candidates for treatment of mild as well as lethal A(H1N1)pdm09 infections has to be demonstrated *in vivo*. Influenza can be modeled in a wide range of animals like mice, ferrets, pigs, nonhuman primates, rats and cotton rats (Barnard, 2009). Due to the moderate costs of the animals as well as their caging and the comparability of the disease to human illness, mice represent a good compromise for anti-influenza studies. During establishment of antiviral mouse models the dynamics of infection of used virus strains has to be characterized quantitatively. Influenza dynamics depends on viral pathogenicity that can be influenced for example by the efficiency of binding to host receptors, induction of apoptosis, or the replication potential of the virus

* Corresponding author.
** Corresponding author. Fax: +49 3641 532 0803.
E-mail address: reinhard.guthke@hki-jena.de (R. Guthke).
[1] These authors contributed equally to this work.

http://dx.doi.org/10.1016/j.biosystems.2014.02.004
0303-2647/

(Tscherne and Garcia-Sastre, 2011). In addition, the virus-induced host immune response can worsen the disease course. In particular, the pro-inflammatory immune response that comprise cytokine as well as chemokine release of infected cells and the attraction of leucocytes can affect negatively the dynamics of infection and contribute to a severe course of influenza (Arankalle et al., 2010; de Castro et al., 2010).

Viral titers (Baccam et al., 2009) or measurements of at least one of the immunological components like interferons, macrophages, NK cells, B cell, T cells (Hancioglu et al., 2006; Handel et al., 2010; Miao et al., 2010; Lee et al., 2009; Pawelek et al., 2012; Saenz et al., 2010) were used as experimental data for modeling influenza kinetics in different hosts with the aim to identify factors explaining the course of illness (Canini and Carrat, 2011) and/or differences in pathogenicity of influenza strains (Wattrang et al., 2003; Smith et al., 2011). As reviewed by Smith and Perelson (2011), there are an increasing number of influenza kinetics models based on viral load data. However, these authors also express their doubts about using viral load as the only indicator of disease severity because immunopathology is discussed as an additional factor in severe infection (de Castro et al., 2010). For example, Kumar et al. (2004) have shown that a strong late immune response can increase the risk of persistent inflammation even after clearing the pathogen. Interestingly, Smith and Perelson (2011) suggest that assigning a symptom score throughout the infection could offer a new perspective into the characteristics of an infection. A symptom score is easily attainable and reflects how sick a host is.

Both small-scale mathematical models (e.g., Saenz et al., 2010; Baccam et al., 2009) and complex models with more than 10 equations and more than 50 parameters (e.g., Hao et al., 2013; Hancioglu et al., 2006; Lee et al., 2009) have been proposed. However, complex models require an increased number and quality of experimental data to calibrate the model parameters. Small-scale models have the advantage to be applicable for quantitative comparison of a (also large) set of experiments (e.g., with different virus strains and/or therapeutic strategies) with a limited experimental effort.

The aim of the present study was to use the symptom score as an easily attainable data source and to develop a small-scale mathematical model of influenza dynamics. Virus pathogenicity, antiviral immune defense, and pro-inflammatory response resulting from viral pathogenicity as well as inflammation were considered as main model variables in a three differential equation model. In the present work, the dynamics of influenza induced by three different A(H1N1)pdm09 strains and one swine H1N2 strain in mice was modeled by a single model with 8 parameters on experimental data given by the symptoms score.

2. 2 Materials and methods

2.1. Cells and viruses

Madin-Darby canine kidney (MDCK) cells (Friedrich-Loeffer Institute, Riems, Germany) were maintained in Eagle's minimum essential medium (EMEM) supplemented with 100 U/ml penicillin and 100 U/ml streptomycin, 10% fetal bovine serum, and 2 mM L-glutamine.

The A(H1N1)pdm09 influenza virus strains A/Jena/5258/09 ('Jena/5258'), A/Jena/5555/09 ('Jena/5555') (Kirchmair et al., 2011; Durrwald et al., 2010), and A/Jena/2688/10 ('Jena/2688') were isolated in MDCK cells from respiratory specimen that originated from patients with clinical symptoms of influenza infection. The European swine H1N2 influenza virus A/swine/Bakum/1832/00 ('Bakum/1832') was obtained from a nasal swab of a diseased pig (Bauer et al., 2012; Schrader and Suss, 2003).

Virus titers were determined by titration of 10-fold serial dilutions on confluent MDCK cells. The 50% tissue culture infectious dose ($TCID_{50}$) was calculated according to Reed and Muench (1938). For isolation, titration and propagation of viruses EMEM formulated with 100 U/ml penicillin and streptomycin, 2 μg/ml trypsin, and 0.1% sodium bicarbonate was used (test medium).

2.2. Animal experiments and data

Experiments were performed in female BALB/c mice (16–18 g; Charles River, Bad Sulzfeld, Germany). After isoflurane anesthesia, five mice were inoculated intranasally with 10^6 $TCID_{50}$/20 μl of each virus in EMEM. Three mice were mock-infected for control. Body weight and clinical score were used as study parameters and monitored for 21 days after virus challenge. Mice that lost more than 25% of their initial body weight were sacrificed. A laboratory clinical score was used to assess the severity of disease. It ranged from 0 to 7: 0 – no changes, 1 – scrubby coat in the neck, 2 – scrubby coat in the neck and on the back, 3 – scrubby coat on whole body, incipient hunchbacked posture, 4 – scrubby coat, hunchbacked posture, incipient inactivity, eyes half closed, 5 – scrubby coat, hunchbacked posture, inactivity, eyes closed, 6 – scrubby coat, hunchbacked posture, completely inactive, eyes closed, 7 – mouse deceased. The mean values and standard deviation (*Std*) for the clinical score (S) as well as the percentage of body weight changes in comparison to day 0 were calculated.

3. Theory and calculations

3.1. Model

The mathematical model representing the within-host influenza dynamics consists of a system of three differential equations in which the dependent variables represent the virus pathogenicity (P), antiviral immune defense (D) including both the innate immune response and the adaptive immune response, and inflammation due to pro-inflammatory response (I). The mathematical equations of our reduced model are:

$$\frac{dP}{dt} = \alpha * P * \left(1 - \frac{P}{k_p}\right) - \beta * D * \frac{P}{P + 0.01} \quad (1)$$

$$\frac{dD}{dt} = y * P - \theta * D \quad (2)$$

$$\frac{dI}{dt} = \varepsilon * f(D) - \rho * I \quad (3)$$

$$f(D) = 1 + \tan\ h\frac{(D - \delta)}{\omega} \quad (4)$$

$$S = P + I \quad (5)$$

The virus pathogenicity P represents the virulence of the virus strains. The dynamics of change of P is described by Eq. (1). It depends on viral infection and the immune response of the host. The first term is parameterized by the virus infection rate (parameterized by α) and the maximum primary pathogenicity (parameterized by k_P). The second term of Eq. (1) represents the efficiency of the early immune response to the virus (parameterized by β). For very small values of P this second term goes to zero due to the Michaelis–Menten function parameterized by a small and fixed Michaelis–Menten constant 0.01 (smaller values or other functions that go to zero if P becomes zero do not change the model behavior) to avoid that P becomes negative.

The antiviral defense is modeled by the variable D including both the innate immune response and the adaptive immune response. Although the defense system is very complex, in the small-scale model the change of the defense system is modeled in Eq. (2) by only

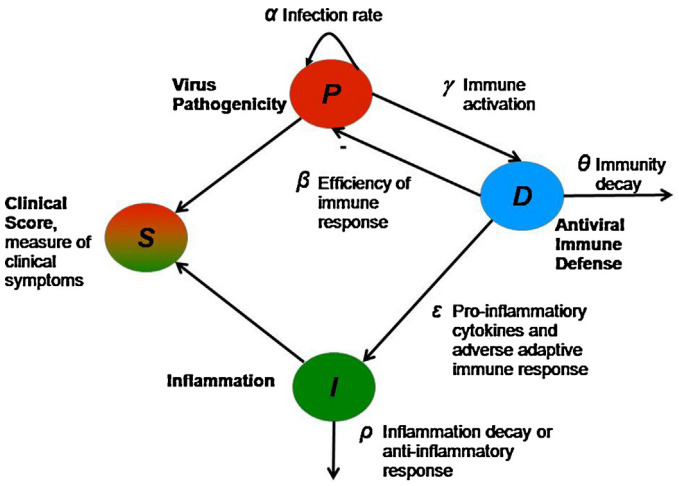

Fig. 1. Model structure. The model variables P (pathogen), D (defense), I (inflammation), and S (clinical score) as well as the relations between them according to Eqs. (1)–(5).

two terms. The first term represents the activation of the defense systems in response to the pathogen (parameterized by γ) and the second term represents the immunity decay (parameterized by θ), which means that once the pathogen has been cleared off from the host system, the defense system should come to rest. Both terms are modeled by first-order reactions.

The third model variable I represents the inflammation due to pro-inflammatory response. Its change is described by Eq. (3). This model formulation is derived from Kumar et al. (2004) and describes a combined effect of cytokines and chemokines, and stimulatory effects of tissue damaged and dysfunction. The first term according to Kumar et al. is a hyperbolic function of antiviral defense system of the host D which strength is parameterized by ε. The parameter δ in Eq. (4) represents the triggering threshold value for the chronic inflammation along with the parameter ω, which represents the strength of prolongation of the inflammation. The ratio δ/ω represents the intensity of the inflammation which can explain whether the virus triggers the chronic inflammation or the acute one. The second term in Eq. (4) represents the relaxation of the inflammation (parameterized by ρ) which could be the anti-inflammatory response by the host. This part of inflammation (denoted by I) does not help in removing the pathogen but leads to collateral damage to the neighboring tissue (Goris et al., 1985; Takala et al., 1999) contributing to the influenza virus-induced symptoms (clinical score S) as modeled by Eq. (5). Fig. 1 displays the model structure and Table 1 lists the model parameters.

3.2. Model simulation and parameter estimation

The model formulated by the Eqs. (1)–(5) is numerically solved using the R-package deSolve from Soetaert et al. (2010). The LSODA method of integration (Petzold, 1983) was employed using a step size of 0.01. The R-package FME from Soetaert et al. (2010) was used for the estimation of parameter values and their impact (sensitivity) on the model output S. The Levenberg–Marquardt algorithm (Moré, 1978) has been used to fit the model variable S to the respective data (observed clinical score) as implemented in the *modFit* function of the package FME. The *modCost* function from the package has been used in the fitting procedure and is the sum of the variable costs, which are scaled according to the number of observations. The variables cost itself is calculated as the sum of squared weighted residuals, where the standard deviation *Std* of the mean of the observed clinical score S is used as weight.

Table 1
Description of model variables and parameters.

Model variables		
t	Time (d)	
P	Virus pathogenicity	
D	Antiviral immune defense	
I	Inflammation due to pro-inflammatory response	
S	Clinical score; measure of clinical symptoms	
Model parameters		**Value**
α	Viral infection rate	Estimated (d^{-1})
k_P	Maximum primary pathogenicity	Estimated
β'	Efficiency of immune response	Fixed: 1 d^{-1} Eliminated, see text
γ	Rate of activation of the immune system	Estimated (d^{-1})
θ	Convalescence rate of immune system; immune decay	Fixed: 0.01 d^{-1} See text
ε	Rate at which inflammation gets activated	Estimated (d^{-1})
δ	Triggering threshold value of the defense for inflammation	Estimated for biphasic course only
ω	Tolerance value of the defense for the chronic inflammation	Estimated for biphasic course only
ρ	Relaxation rate of inflammation/Anti-inflammatory response	Fixed: 1.82 d^{-1}, Canini and Carrat, 2011
$P(0)$	Virus pathogenicity, initial value	Fixed: 0.01 Baccam et al. (2009)
$D(0)$	Antiviral immune defense, initial value	Fixed: 0.00
$I(0)$	Inflammation due to pro-inflammatory response, initial value	Fixed: 0.00

Finally, a Markov Chain Monte Carlo (MCMC; implemented in the package FME; Soetaert and Petzoldt, 2010) simulation was used to estimate the uncertainty of the parameter estimates as resulted by the model fit. The first 500 iterations were removed which is known as burn-in so as to make sure the chain was close enough to target distribution. The parameters sets that gave the highest probability to fit the model have been chosen as the final parameter sets for the model fitting. All the parameter values and variables are positive.

3.3. Parameter sensitivity analysis

The sensitivity and identifiability analysis were done by the functions *sensFun* and *collin* outlined in the R-package FME. Briefly, this is done by estimating at each data point the derivative of the clinical score S with respect to the parameter values p_j. The sensitivities are dimensionless, as they are scaled with respect to the variables and parameter values:

$$\Sigma_i = \frac{p_j}{S}\frac{\partial S}{\partial p_j} \tag{6}$$

These sensitivities allow to determine which parameter is least important to the model output and these least sensitive parameters can be fixed and not used for calibration.

3.4. Parameter identifiability analysis

Raue et al. (2009) distinguished between structural and practical identifiability. A structural identifiability analysis gives insight into which parameters can be simultaneously estimated, given noise-free data and a model that can fit the data perfectly. A structural non-identifiability is caused by redundant parameterization. Here, the structural identifiability was evaluated by investigating the

Table 2
Model parameter values. Parameter values and their 95% confidence intervals (in brackets) identified by model fit to the observed clinical scores. The parameter values NaN denote that they could not be identified. Units of the parameters are displayed in Table 1.

Strain/parameter	Infection experiments			
	Jena/5258 (A(H1N1)pdm09)	Jena/5555 (A(H1N1)pdm09)	Jena/2688 (A(H1N1)pdm09)	Bakum/1832 (swine H1N2)
α	3.63 [3.62, 5.78]	3.64 [3.31, 4.16]	2.12 [2.03, 2.29]	2.22 [2.09, 2.40]
k_P	3.23 [2.31, 3.29]	5.69 [5.13, 6.17]	3.72 [3.02, 4.54]	4.85 [4.27, 5.36]
γ'	0.51 [0.25, 0.64]	0.28 [0.27, 0.31]	0.52 [0.44, 0.65]	0.29 [0.24, 0.32]
θ	0.01	0.01	0.01	0.01
ε	6.81	0	0	0
δ'	4.27	NaN	NaN	NaN
ω'	0.13	NaN	NaN	NaN
ρ	1.82	1.82	1.82	1.82

pairwise linear dependence or collinearity of all possible parameters sets. If the 'collinearity index' calculated by the function *collin* exceeds a critical values typically chosen to be 10–15, then the parameter set is regarded as poorly identifiable (Brun et al., 2001).

In practice, all measurements have error and the model is non-perfect and this causes the uncertainty of the parameters values characterized by confidence regions. The practical non-identifiability is characterized by an infinitely extended confidence region in increasing and/or decreasing direction. For the estimation of confidence intervals the data-dependent probability distribution of the parameters have to be derived. Raue et al. introduced the profile likelihood to estimate the confidence intervals. In the present work, a Bayesian method, in particular the Markov Chain Monte Carlo approach using the DRAM method (Delayed Rejection Adaptive Metropolis) (Haario et al., 2006) as implemented in FME was applied to visualize the confidence regions by pairwise scatter plots and to estimate the confidence intervals.

4. Results

The parameter β was eliminated by the following model transformation: $\beta' = 1\,d^{-1}$, $D' = D * \beta$, $\gamma' = \beta * \gamma$, $\delta' = \delta * \beta$, $\omega' = \omega * \beta$. In the following text, the transformed parameters are used for better readability without the prime. Then, the mathematical model includes 8 parameters, four of them (α, γ, k_p, ε) were virus strain specific and therefore calibrated individually by fitting to the data of the experiments with different virus strains. The two parameters δ and ω are only relevant for biphasic course of infection and, thus, estimated only for the virus Jena/5258. The remaining two parameters ρ and θ are host-related and, therefore, fixed, i.e., identical for the four virus strains. For the inflammation decay ρ we use the value $1.82\,d^{-1}$ published by Canini and Carrat (2011). The fixed parameter θ were calculated by model fit to all the data sets providing a rich data set of 72 data points from four different virus strains. The values of the fixed parameters are shown in Table 1.

Fig. 2 displays the results of model fit to four experimental viral infections with four different virus strains. Table 2 depicts the identified values of the 8 model parameters (i.e., all but the eliminated parameter β) together with their 95% confidence intervals.

The mean sensitivity values (averaged over time) of the model parameters calculated by Eq. (6) for the four virus strains are shown in Table 3. As displayed in Table 3, we used different time intervals for averaging to exclude periods with values of S close to zero as S is in the denominator in Eq. (6). The temporal profiles of the sensitivity are depicted in the Supplementary Fig. S4.

For Jena/5258, the threshold parameter δ is the most sensitive model parameter. Here, the immune defense (D) exceeds the threshold parameter δ and triggers the onset of inflammation due to the fact that three parameters are high: (i) α, i.e., the viral replication and infection rate, (ii) γ, i.e. the rate of early activation of the immune system, and (iii) the parameter ε, i.e., the rate at which inflammation gets activated. For Jena/5258, the parameter k_P called maximum primary pathogenicity is the second most sensitive parameter after the threshold parameter δ. The infection with this strain is characterized by the highest clinical score value that is caused not by a high primary pathogenicity k_P but by the inflammation ('secondary pathogenicity'). This parameter k_P has the smallest value of 3.23 for Jena/5258 and the highest value of 5.69 for Jena/5555. The confidence intervals (CI) of k_P for these two virus strains with high temporal maximum clinical score are disjunctive, i.e., without overlap. Thus, the causes of high clinical score in both infection courses are different: Jena/5555 causes the high clinical score by a high primary pathogenicity, while Jena/5258 by high inflammation.

The parameter α called viral infection rate is the next most sensitive parameter for Jena/5258 with biphasic course of infection, but the most sensitive parameter for the other three virus strains with monophasic profile (Table 3). It has the highest identified values for the H1N1 strains Jena/5258 and Jena/5555 that are characterized by the utmost clinical score. The CI of α for these two virus strains are disjunctive to the respective intervals of the other two virus strains Jena/2688 and Bakum/1832.

For all four virus strains, the parameter γ, which quantifies the rate of activation of the immune system, is the third (fourth for Jena/5258) most sensitive parameter – after k_p and α (and after δ that is only relevant for the strain Jena/5258). Parameter γ has the highest value of 0.52 for Jena/2688 where the corresponding CI is disjunctive to the respective intervals of the strains Jena/5555 and Bakum/1832 with estimated parameter values smaller than 0.3.

In Table 2, the confidence intervals are only shown for the parameters α, γ and k_p. The distribution and the pairwise scatter plot of the MCMC-generated parameter values shown in Figs. 3 and 4 give a hint to the practical identifiability of these three most important model parameters.

The parameters ε, i.e., the rate at which inflammation gets activated, as well as ω and δ were only identified for Jena/5258 that exhibits a biphasic course of infection. For the other three strains the kinetics of inflammation is non-observable based on the measured clinical score S and the model Eqs. (1)–(5). Therefore, the

Table 3
Sensitivities of the model parameters. Mean value (averaged over time) of the sensitivity with respect to the read out value S.

Strain/Parameter	Infection experiments			
	Jena/5258	Jena/5555	Jena/2688	Bakum/1832
Time interval (d)	[0,10]	[0,5]	[0,5]	[0,5]
α	2.88	0.99	1.78	1.67
k_P	4.57	0.39	0.46	0.46
γ'	0.96	−0.12	−0.34	−0.16
θ	0.38	0.00	0.01	0.01
ε	0.20	0	0	0
δ'	−8.03	0	0	0
ω'	0.00	0	0	0
ρ	−0.46	0	0	0

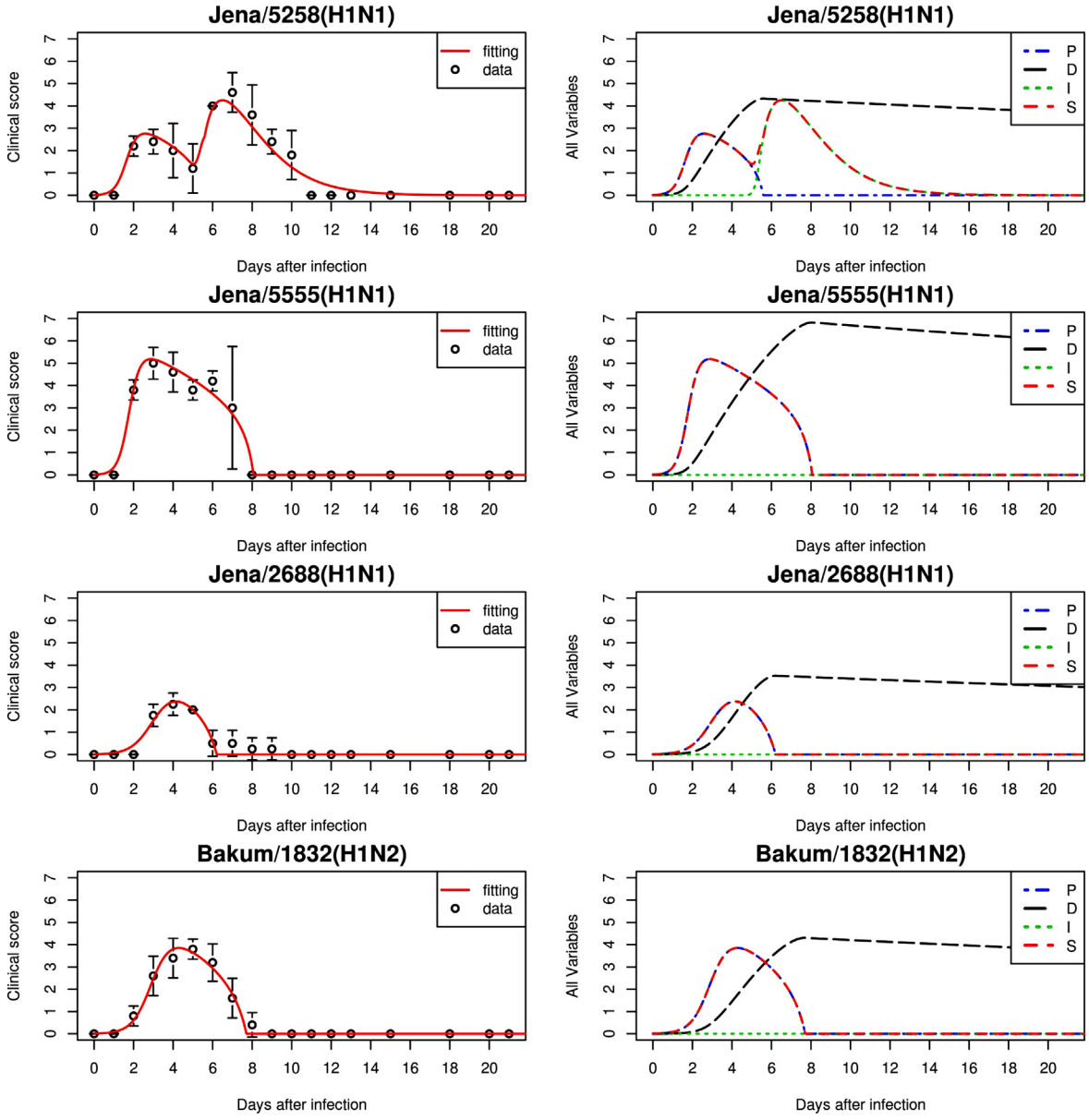

Fig. 2. Model fit to the clinical score after infection with four different virus strains. Top: A(H1N1)pdm09 Jena/5258; medium: A(H1N1)pdm09 Jena/5555 and A(H1N1)pdm09 Jena/2688; bottom: European swine H1N2 Bakum/1832; all infected with 10^6 $TCID_{50}$/mice; black circles: observed and averaged clinical score S; bars: '*Std*' (standard deviation); red lines: model kinetics S as simulated using Eqs. (1)–(5); blue dashed lines: model variable P; black dashed lines: model kinetics D'; green dotted lines: model kinetics I. (For interpretation of the references to color in text, the reader is referred to the web version of this article.)

parameter ε was set to zero and the parameter values ω and δ were denoted in Table 2 as unknown for the infection experiments using the virus strains Jena/5555, Jena/2688, and Bakum/1832.

The model parameters k_P, α, *and* γ were found to be the most discriminative and identifiable parameters that quantitatively characterize the four virus strains under investigated in this study. Each of the four virus strains is characterized by a specific pattern with respect to these three parameters as displayed in Table 4.

Table 4
Virus-specific pattern with respect to three model parameters. Labels 'low' versus 'high' represent disjunctive confidence intervals of the respective parameter values.

Strain/parameter	Infection experiments			
	Jena/5258	Jena/5555	Jena/2688	Bakum/1832
k_P	Low	High	(Medium)	(Medium)
α	High	High	Low	Low
γ'	(Medium)	Low	High	Low

To evaluate the structural identifiability of the non-fixed parameters, the collinearity index (also known as condition number) was estimated using the function *collin* of the R-package FME. The collinearity indices for all combinations of the 8 model parameters α, k_P, γ, θ, ε, δ, ω, and ρ are high (Supplementary Fig. S1) and, thus, demonstrate the structural non-identifiability of the whole parameter set. The collinearity indices for the combinations of the three most important model parameters α, k_P, and γ are shown in the Supplementary Fig. S2. These values are below 5. As a rule of thumb, a collinearity index less than 10–15 estimated by the function *collin* of the R-package FME is assumed to be structural identifiable (Brun et al., 2001). Figs. 3, 4 and S3 show the scatter-plot matrices visualizing the model parameter values from MCMC-generated samples, the probability distribution of the model parameters values and their pair-wise correlation coefficients as calculated by the function *pairs* of the package FME. For all four experiments the distributions of the parameters α, k_P, and γ tend to zero for both increasing as well as decreasing values and the correlation between the

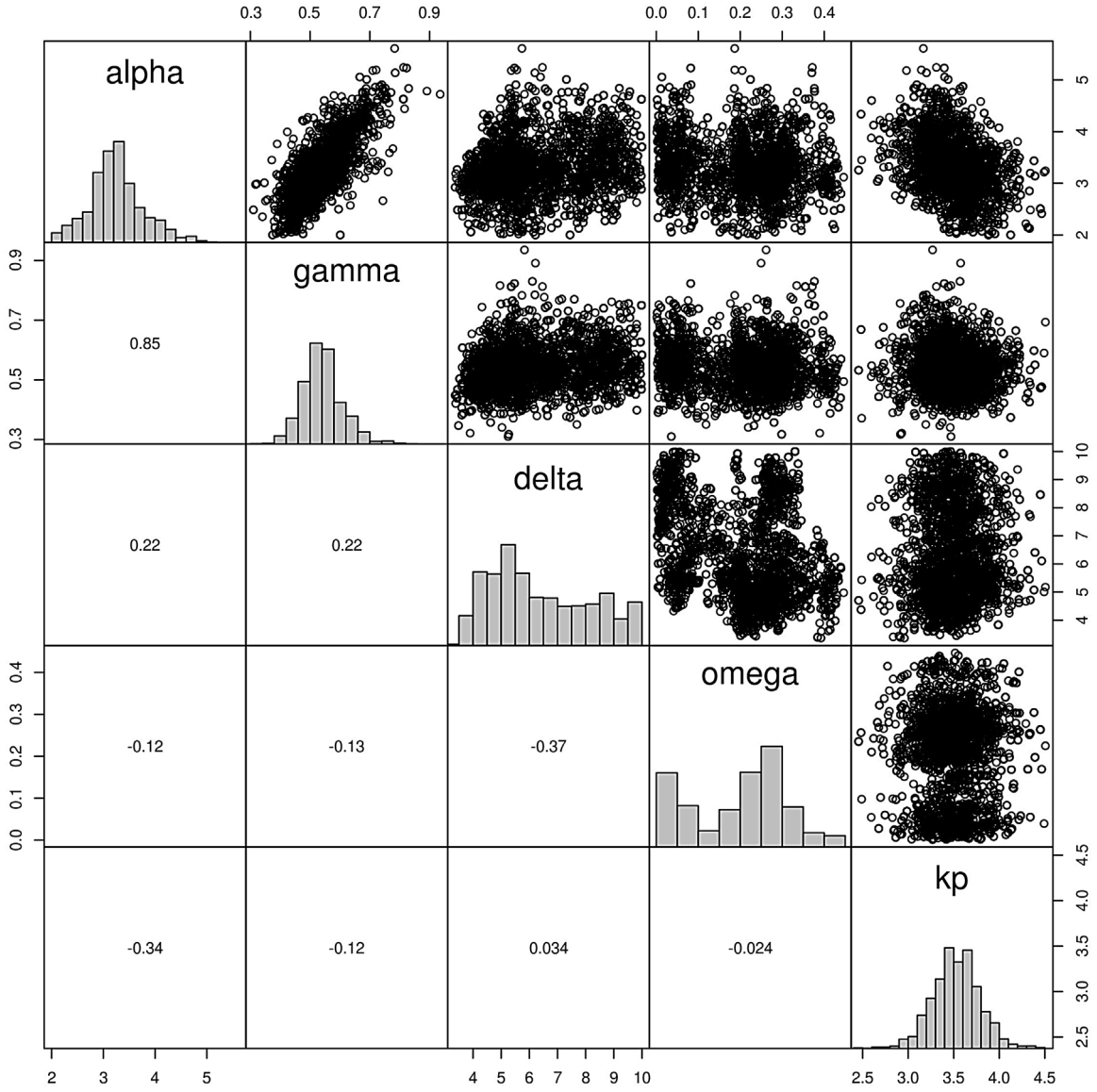

Fig. 3. Scatter-plot of the Markov Chain Monte Carlo (MCMC) samples for the virus strain Jena/5258. The top right panels show the pair-wise plot of the parameters α, γ, δ, ω, and k_P. For the total parameter set see Supplementary Fig. S3. The range of the parameters is shown at the outer axis; 1000 random parameter sets around the parameter set calibrated for Jena/5258. The probability distribution for each parameter is shown in the diagonal panels. The bottom panels give the correlation coefficients for each parameter pair.

parameter values is low, i.e., the highest absolute value of correlation coefficients is 0.86. That indicates, that the confidence regions are finite and these three parameters are obviously practically identifiable based on the measured data of all the four experiments studied. The remaining parameters are non-identifiable at all and, therefore, they were fixed in our study. The parameters ε, δ, and ω were estimated as displayed in Table 2 for the infection with virus strain Jena/5258 that shows biphasic course. The distributions of these parameters do not show finite borders in both Figs. 3 and S3. For the other three virus strains with a monophasic course, the parameter ε were set to zero and the values of the parameters δ and ω are irrelevant as inflammation does not cause a separate peak in the profile of the clinical score S and, therefore, it is non-observable based on these easily attainable experimental data.

The parameter ε quantifies the degree of damage caused by the adverse effect of inflammation with respect to individual virus strains. The high values of the three parameters α, γ and ε could explain the biphasic course of clinical symptoms after infection with the virus strain Jena/5258 by stronger inflammation reaction.

Fig. 5 visualizes that the body weight is negatively correlated to the clinical score S as shown in Fig. 2. This observation supports the assumption implemented in the model Eqs. (1)–(5) that the second peak of S for Jena/5258 is caused by inflammation processes (represented by the model variable I) which is responsible for damage and the loss of body weight of the infected mice.

5. Discussion

The main focus of this study was to quantify the kinetics of influenza caused by different viral strains based on a single model by only few most important parameters. With this aim, a dynamic model of influenza in mice was established and fitted to experimental data representing virus-induced clinical symptoms. Three non-fixed model parameters were proven to be identifiable and to be suitable to quantitatively characterize the four different virus strains under study: (i) the viral replication and infection rate (α), (ii) the maximum primary pathogenicity (k_p), and (iii) the rate of early activation of the immune system (γ). However, the

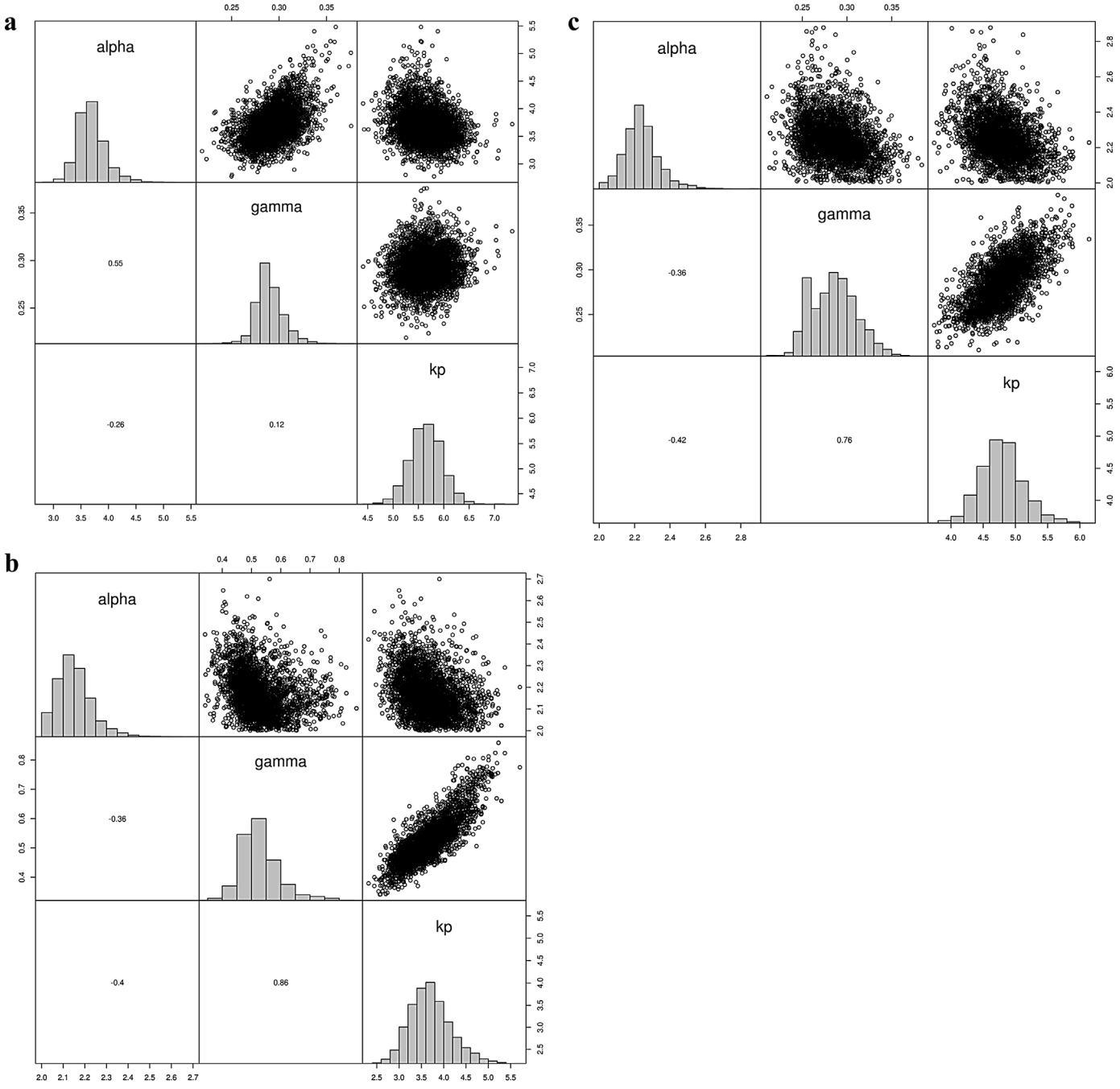

Fig. 4. Scatter-plot of the Markov Chain Monte Carlo (MCMC) samples for the virus strains Jena/5555 (top), Jena/2688, and Bakum/1832 (bottom).

model structure is hypothetic. Follow-up experiments including molecular parameters and genome-wide transcriptome analysis are ongoing to discriminate between alternative models and to verify the hypothesis that the second peak of biphasic course of infection is caused mainly by inflammation. Thus, the models suggested in the present study describe the course of influenza based on virus infection and on virus-induced immune response including pro- as well as anti-inflammatory response. Finally, they link the virus pathogenicity and/or inflammation with the observable clinical symptoms.

The small-scale model has some interesting features: First, it is able to describe the outcome of infection with four influenza virus strains. Thus, the model can be used to quantify the virulence of different strains by a set of 8 parameters listed in Tables 1 and 2. Three of them (α, k_P, γ) were found to be structurally as well as practically identifiable. The remaining five parameters are non-identifiable with the given experimental data. They were fixed, which is no critical for four of them due to their low sensitivity. Only for the threshold parameter δ introduced by Kumar et al. (2004), the practical non-identifiability is an issue for further studies due to its high sensitivity for biphasic profiles of the clinical score.

Second, the model is able to simulate and interpret the cause of different outcomes of disease after virus challenge in mice. At day 2 p.i. mice became ill independently from the virus strain and infection dose studied. Maximum clinical score was observed between days 3 and 6 after infection with Jena/5555, Bakum/1832, and Jena/2688; afterwards mice recovered (monophasic kinetic). Also there is only low or no persistent inflammation. Obviously, the

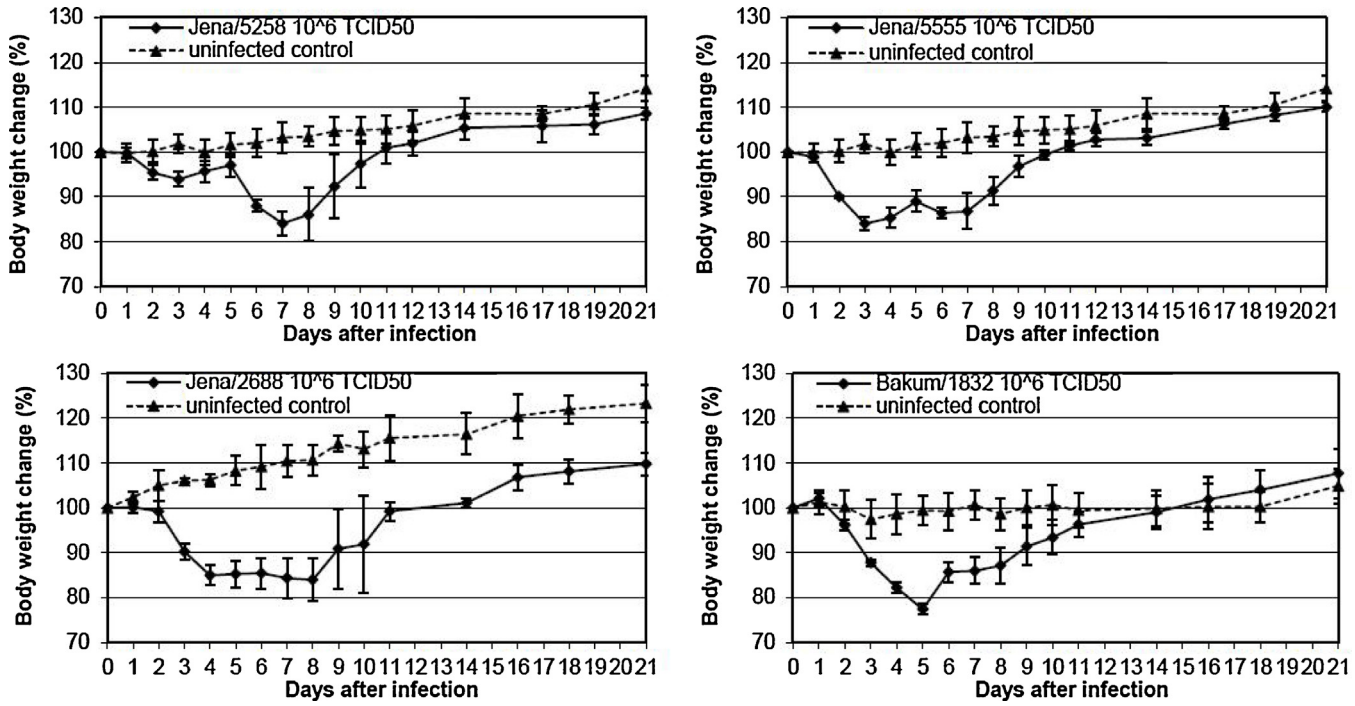

Fig. 5. Body weight change after infection with four different virus strains. *Top left*: A(H1N1)pdm09 Jena/5258; *Top right*: A(H1N1)pdm09 Jena/5555; bottom left: (H1N1)pdm09 Jena/2688; bottom right: European swine H1N2 Bakum/1832 (full squares) compared with uninfected mice (triangles).

respective viruses have been eliminated efficiently by the immune response. In contrast, after infection with Jena/5258, a biphasic course of clinical symptoms were observed and simulated by the mathematical model. According to the established model, persistent inflammation contributes to the biphasic course of disease. Due to the experimental design, it remains unclear whether the virus was eliminated or not at the second peak of disease. So there is still an open question, whether the second peak of the disease is solely due to the persistent inflammation or due to the existence of mutant influenza virus.

For modeling of the biphasic behavior, a dynamic model introduced and theoretically studied by Kumar et al. (2004) was used and reduced. To the best of knowledge, in the present work, the first time Kumar's model was fitted to experimental data by linking the strength of inflammation with the clinical score that monitors clinical symptoms representing influenza in mice. In addition, the course of infection of the A(H1N1)pdm09 virus as well as a European swine H1N2 influenza virus (Bakum/1832) was modeled the first time.

Based on the model presented here, it can be assumed that the dynamics of influenza depends on both the virus pathogenicity as well as the adverse adaptive immune response that includes the pro-inflammatory cytokines (Pommerenke et al., 2012; Arankalle et al., 2010). Arankalle et al. (2010) showed the absence of viremia in both critically ill patient and mild patients infected with A(H1N1)pdm09 virus suggesting that viral replication may not be the major factor for the observed differences in the course of influenza disease. Based on the determined significantly increased levels of several chemokines and pro-inflammatory cytokines that may result in massive infiltration of leucocytes, these authors suggest that excessive damage resulting from immune response may also contribute to disease severity.

This supports the model predictions where a higher severity and inflammatory reaction was seen in one of the virus strain used.

The model established in the present study is able to interpret and quantify the biphasic course of disease by a late inflammation phase. It allows quantifying the rate of pro- and anti-inflammatory response (ε and ρ, respectively) as well as the conditions for the onset of inflammation (δ, ω) by a set of identified parameters. As suggested already by Kumar et al. (2004), it was hypothesized with Eqs. (3) and (4) that the onset of inflammation (model variable I) is triggered by the immune defense (if the model variable D goes beyond the threshold value δ). The sensitivity of the pro-inflammatory response in dependence on the immune defense is quantified by the parameter ($1/\omega$). These results warranted a more detailed biological characterization of pro-inflammatory response that is ongoing now. As published recently for a non-lethal infection of C57BL/6J mice with A/Puerto Rico/8/34 (Pommerenke et al., 2012), a transcriptome analysis will help to clarify the role of factors of innate and adaptive host immune response in severe biphasic influenza in mice.

The observed clinical score was used for the presented model fit. These data are negatively correlated with the body weight (W; Fig. 5). Thus, the body weight could be used alternatively for model fit using a linear regression model ($W = \mathrm{W}_0 - \mathrm{a} * P - \mathrm{b} * I$).

The model introduced by Canini and Carrat (2011) was based on population analysis of viral kinetics and symptoms dynamics which is similar to our study. The major limitation with their model was that data of immune response were not included. Their model was solely dependent on the pathogenicity of virus used. They assume that natural killer cells contribute to adverse inflammation which supports the hypothesis of the small scale model of the present study. In addition, the suggestion of Smith and Perelson (2011) to use clinical score as easily attainable experimental data supports the approach used here.

The established model may help to quantify the dynamics of influenza induced by different virus strains and support the search for reasons for the severe, biphasic course of influenza in mice. Including antiviral treatment, drug administration could be optimized specifically for the virus strain used in further studies. The model might allow to direct antiviral studies including the mathematical analysis of the use of antiviral compounds such as oseltamivir for the treatment of pandemic influenza virus

infections (as modeled e.g., for the therapy HIV therapy by Pitchaimani et al. (2013)).

6. Conclusion

In the current study, a small-scale mathematical model of pandemic H1N1(2009) influenza A (A(H1N1)pdm09) infection was developed with a special emphasis on the late pro-inflammatory response. Simulation analysis of this model revealed that the pro-inflammatory response plays some adverse role on the disease condition. For the first time, the dynamics of four different influenza A virus strains (three A(H1N1)pdm09 and one European swine H1N2) were modeled. The established model allows quantifying the infection process by using a few interpretable parameters. This quantification includes the pathogenicity of different viral strains and the conditions and rate of pro- and anti-inflammatory response. Thus, the model will be important for the quantitative comparison of virus strains as well as condition for different outcome of the infection process. Most importantly, the main focus was to quantify the kinetics of different viral strains based on single model. The model study shows, that the inflammatory response is specific for the virus strain and, thus, it plays a crucial role for optimization of the therapeutic profile of drug administration that should be designed specifically for the virus strain. Due to the lack of additional experimental data, viral adaptation cannot be excluded as additional risk factor for biphasic influenza. Taken together, the models can be easily used to quantify influenza disease caused by different influenza virus strains and give hints for the experimental setup to further analyze the driving factors for severe disease as well a drug susceptibility.

Acknowledgments

This study was supported by grant of the German Federal Ministry of Education and Research (01 K1 1006J) as well as the European Social Fund and the Thuringia Ministry of Economy, Technology, and Work (2011 FGR0137).

Appendix A. Supplementary data

Supplementary data associated with this article can be found, in the online version, at http://dx.doi.org/10.1016/j.biosystems.2014.02.004.

References

Arankalle, V.A., Lole, K.S., Arya, R.P., Tripathy, A.S., Ramdasi, A.Y., Chadha, M.S., Sangle, S.A., Kadam, D.B., 2010. Role of host immune response and viral load in the differential outcome of pandemic H1N1 (2009) influenza virus infection in Indian patients. PLoS ONE 5 (10), e13099.

Baccam, P., Beauchemin, C., Macken, C.A., Hayden, F.G., Perelson, A.S., 2009. Kinetics of influenza A virus infection in Human. J. Virol. 80 (15), 7509–7590.

Barnard, D.L., 2009. Animal models for the study of influenza pathogenesis and therapy. Antiviral. Res. 82 (2), A110–A122.

Bauer, K., Durrwald, R., Schlegel, M., Pfarr, K., Topf, D., Wiesener, N., Dahse, H.M., Wutzler, P., Schmidtke, M., 2012. Neuraminidase inhibitor susceptibility of swine influenza A viruses isolated in Germany between 1981 and 2008. Med. Microbiol. Immunol. 201, 61–72.

Brun, R., Reichert, P., Kunsch, H., 2001. Practical identifiability analysis of large environmental simulation models. Water Resour. Res. 37 (4), 1015–1030.

Canini, L., Carrat, F., 2011. Population modeling of influenza A/H1N1 virus kinetics and symptoms dynamics. J. Virol. 85, 2764–2770.

Dawood, F.S., Jain, S., Finelli, L., Shaw, M.W., Lindstrom, S., Garten, R.J., Gubareva, L.V., Xu, X., Bridges, C.B., Uyeki, T.M., Novel Swine-Origin Influenza A (H1N1) Virus Investigation Team, 2009. Emergence of a Novel Swine-Origin Influenza A (H1N1) virus in humans. N. Engl. J. Med. 360 (25), 2605–2615.

de Castro, I.F., Guzmán-Fulgencio, M., García-Alvarez, M., Resino, S., 2010. First evidence of a pro-inflammatory response to severe infection with influenza virus H1N1. Crit. Care 14, 115.

Durrwald, R., Krumbholz, A., Baumgarte, S., Schlegel, M., Vahlenkamp, T.W., Selbitz, H.J., Wutzler, P., Zell, R., 2010. Swine influenza A vaccines, pandemic (H1N1) 2009 virus, and cross-reactivity. Emerg. Infect. Dis. 16, 1029–1030.

Ginsberg, M., Hopkins, J., Maroufi, A., Dunne, G., Sunega, D.R.<ET-Al>, 2009. Swine influenza A (H1N1) infection in two children – Southern California, March–April 2009. MMWR Morb. Mortal Wkly. Rep. 58 (15), 400–402.

Goris, R.J., te Boekhorst, T.P., Nuytinck, J.K., Gimbrere, J.S., 1985. Multiple-organ failure: generalized autodestructive inflammation? Arch. Surg. 120, 1109–1115.

Gubareva, L., Okomo-Adhiambo, M., et al., 2009. Update: drug susceptibility of swine-origin influenza A (H1N1) viruses, April 2009. MMWR Morb. Mortal Wkly. Rep. 58 (16), 433–435.

Hao, L., Jiang, G., Liu, S., Ling, L., 2013. Global dynamics of SIRS epidemic model with saturation incidence. Biosystems 114 (1), 56–63.

Hancioglu, B., Swigon, D., Clermont, G., 2006. A dynamical model of human immune response to influenza A virus infection. J. Theor. Biol. 246 (1), 70–86.

Handel, A., Longini, I.M., Antia, R., 2010. Towards a quantitative understanding of the within-host dynamics of influeza A infections. J. R. Soc. Interface 7 (42), 35–47.

Haario, H., Laine, M., Mira, A., Saksamn, E., 2006. DRAM: efficient adaptive MCMC. Stat. Comput. 16, 339–354.

Kao, R.Y., Yang, D., Lau, L.S., Tsui, W.H., Hu, L., Dai, J., Chan, M.P., Chan, C.M., Wang, P., Zheng, B.J., Sun, J., Huang, J.D., Madar, J., Chen, G., Chen, H., Guan, Y., Yuen, K.Y., 2010. Identification of influenza A nucleoprotein as an antiviral target. Nat. Biotechnol. 28 (6), 600–605.

Kirchmair, J., Rollinger, J.M., Liedl, K.R., Seidel, N., Krumbholz, A., Schmidtke, M., 2011. Novel neuraminidase inhibitors: identification, biological evaluation and investigations of the binding mode. Future Med. Chem. 3 (4), 437–450.

Kumar, R., Clermont, G., Vodovotz, Y., Chow, C.C., 2004. The dynamics of acute inflammation. J. Theor. Biol. 230, 145–155.

Lee, H.Y., Topham, D.J., Park, S.Y., Hollenbaugh, J., Treanor, J., Mosmann, T.R., Jin, X., Ward, B.M., Miao, H., Holden-Wiltse, J., Perelson, A.S., Zand, M., 414 Wu, H., 2009. Simulation and prediction of the adaptive immune response to influenza A virus infection. J. Virol. 83, 7151–7165.

Li, Q., Qi, J., Zhang, W., Vavricka, C.J., Shi, Y., Wie, J., Feng, E., Shen, J., Chen, J., Liu, D., He, J., Yan, J., Liu, H., Jiang, H., Teng, M., Li, X., Gao, G.F., 2010. The 2009 pandemic H1N1 neuraminidase N1 lacks the 150-cavity in its active site. Nat. Struct. Mol. Biol. 17 (10), 1266–1268.

Moré, J.J., 1978. The Levenberg–Marquardt algorithm: implementation and theory. In: Watson, G.A. (Ed.), Numerical Analysis, Dundee 1977. Lecture Notes Math. 630, 105–116.

Miao, H., Hollenbaugh, J.A., Zand, M.S., Holden-Wiltse, J., Mosmann, T.R., Perelson, A.S., Wu, H., Topham, D.J., 2010. Quantifying the early immune response and adaptive immune response kinetics in mice infected with influenza A virus. J. Virol. 84 (13), 6687–6698.

Nguyen, H.T., Fry, A.M., Gubareva, L.V., 2012. Neuraminidase inhibitor resistance in influenza viruses and laboratory testing methods. Antivir. Ther. 17 (1 Pt B), 159–173.

Pawelek, K.A., Huynh, G.T., Quinlivan, M., Cullinane, A., Rong, L., Perelson, A.S., 2012. Modeling within-host dynamics of influenza virus infection including immune responses. PLoS Comput. Biol. 8 (6), e1002588.

Petzold, L.R., 1983. Automatic selection of methods for solving Sti and Nonsti systems of ordinary differential equations. SIAM J. Sci. Stat. Comput. 4, 136–148.

Pitchaimani, M., Monica, C., Divya, M., 2013. Stability analysis for HIV infection delay model with protease inhibitor. Biosystems 114, 118–124.

Pommerenke, C., Wilk, E., Srivastava, B., Schulze, A., Novoselova, N., Geffers, R., Schughart, K., 2012. Global transcriptome analysis in influenza-infected mouse lungs reveals the kinetics of innate and adaptive host immune responses. PLoS ONE 7 (7), e41169.

Raue, A., Kreutz, C., Maiwald, T., Bachmann, J., Schilling, M., Klingmüller, U., Timmer, J., 2009. Structural and practical identifiability analysis of partially observed dynamical models by exploiting the profile likelihood. Bioinformatics 25, 1923–1929.

Reed, L.J., Muench, H., 1938. A simple method of estimating fifty percent endpoints. Am. J. Hyg. 27 (3), 493–497.

Saenz, R.A., Quinlivan, M., Elton, D., Macrae, S., Blunden, A.S., Mumford, J.A., Daly, J.M., Digard, P., Cullinane, A., Grenfell, B.T., McCauley, J.W., Wood, J.L., Gog, J.R., 2010. Dynamics of influenza virus infection and pathology. J. Virol. 84 (8), 3974–3983.

Schrader, C., Suss, J., 2003. Genetic characterization of a porcine H1N2 influenza virus strain isolated in Germany. Intervirology 46, 66–70.

Smith, A.M., Adler, F.R., McAuley, J.L., Gutenkunst, R.N., Ribeiro, R.M., McCullers, J.A., Perelson, A.S., 2011. Effect of 1918 PB1-F2 expression on influenza A virus infection kinetics. PLoS Comput. Biol. 7 (2), e1001081.

Smith, A.M., Perelson, A.S., 2011. Influenza A virus infection kinetics: quantitative data and models. Syst. Biol. Med. 3, 429–445.

Soetaert, K., Petzoldt, T., Woodrow, R., Setzer, R.W., 2010. Solving differential equations in R: package deSolve. J. Stat Softw. 33 (9), 1–25.

Soetaert, K., Petzoldt, T., 2010. Inverse modeling, sensitivity and Monte Carlo analysis in R using FME package. J. Stat. Softw. 33 (3), 1–28.

Takala, A., Jousela, I., Jansson, S.E., Olkkola, K.T., Takkunen, O., Orpana, A., Karonen, S.L., Repo, H., 1999. Markers of systemic inflammation predicting organ failure in community-acquired septic shock. Clin. Sci. (Lond.) 97, 529–538.

Tscherne, D.M., Garcia-Sastre, A., 2011. Virulence determinants of pandemic influenza viruses. J. Clin. Invest. 121 (1), 6–13.

Wattrang, E., Jessett, D.M., Yates, P., Fuxler, L., Hannant, D., 2003. Experimental infection of ponies with equine influenza A2 (H3N8) virus strains of different pathogenicity elicits varying interferon and interleukin-6 responses. Viral Immunol. 16 (1), 57–67.

WHO, 2013. Influenza Update No. 184.